CANCER BIOLOGY & THERAPY
2016, VOL. 17, NO. 4, 381–389
http://dx.doi.org/10.1080/15384047.2016.1139229

Taylor & Francis
Taylor & Francis Group

RESEARCH PAPER

# Triptolide mitigates radiation-induced pulmonary fibrosis via inhibition of axis of alveolar macrophages-NOXes-ROS-myofibroblasts

Chun Chen[a,*], Shanmin Yang[b,*], Mei Zhang[b], Zhenhuan Zhang[b], Jingshen Hong[c,d], Deping Han[c,d], Jun Ma[b], Steven B. Zhang[b], Paul Okunieff[b], and Lurong Zhang[b,c,d]

[a]Department of Pharmacology, College of Pharmacy, Fujian Medical University, Fuzhou, China; [b]Department of Radiation Oncology, University of Florida, Gainesville, FL, USA; [c]The First Affiliated Hospital of Fujian Medical University, Fuzhou, China; [d]Key Lab of Radiation Biology, Fujian Medical University, Fuzhou, China

**ABSTRACT**

Purpose: IR-induced pulmonary fibrosis is one of the most severe late complications of radiotherapy for lung cancer. It is urgently needed to discover a new drug for anti-IR lung fibrosis. Our previous studies have indicated that TPL exhibits both anti-IR lung fibrosis and anti-tumor activities. To reveal the mechanism of TPL on anti-IR lung fibrosis, alveolar macrophages (AMs) were examined for TPL effect on their axis of Nicotinamide adenine dinucleotide phosphate oxidase-reactive oxygen species (NOXes-ROS) and myofibroblast activation. Methods and Materials: The fibrosis-prone C57BL/6 mice were irradiated with 15 Gy on whole chest, then one day later, mice were treated without or with TPL (i.v. 0.25 mg/kg, qod for 1 month). The AMs were collected from bronchoalveolar lavage fluids and studied for the production of ROS and the levels of NOXes. The effect of AMs on myofibroblast activation as labeled with F4/80 or $\alpha$-SMA ($\alpha$-smooth muscle actin) were examined using flow cytometry, Western blotting, or immunohistochemical staining. Results: TPL effectively reduced the IR-induced lung fibrosis as evidenced by the less myofibroblasts, less collagen deposit and less ROS in the IR-lung tissues. We found that ROS which responsible for myofibroblasts activation was mainly from AMs and was NOX2 and NOX4 dependent. TPL significantly reduced the infiltrated AMs in IR-lung tissues, and in addition, down regulated the level of NOX2 and NOX4 in AMs both *in vitro* and *in vivo*. Furthermore, by inhibiting NOXes dependent ROS in AMs, TPL deprived AMs' paracrine activation of myofibroblasts. Conclusions: Our work demonstrated that the anti-fibrotic effect of TPL on IR-induced pulmonary fibrosis was related to its inhibition on the axis of alveolar macrophages-NOXes-ROS-myofibroblasts.

**ARTICLE HISTORY**
Received 12 August 2015
Revised 8 December 2015
Accepted 1 January 2016

**KEYWORDS**
Alveolar macrophages; myofibroblasts; NOXes; pulmonary fibrosis; radiation; ROS; Triptolide

## Introduction

Pulmonary fibrosis, a severe late complication after thoracic radiotherapy, leads to permanent scarring in the lung and greatly reduces the quality of patients' life. So far, there is no effective medication for it.[1]

Clearly, an anti-fibrotic agent with a defined action mechanism is urgently needed. Our previous studies and others have shown that TPL, a diterpenoid epoxide purified from the *Tripterygiumwilfordii Hook F*, exhibits both anti-inflammation and anti-tumor activities. It has been used to treat bleomycin-induced pulmonary fibrosis,[2,3] liver fibrosis[4] and renal fibrosis [5] in mice. Although we found that TPL alleviated IR-induced pulmonary fibrosis in C57BL/6 mice,[6] its underlying mechanism remains unknown.

The activation and persistence of myofibroblasts are the core events of pulmonary fibrosis. Fibroblasts can be activated and transformed into myofibroblasts, and $\alpha$-SMA expression and increased matrix production were the marker of myofibroblasts.[7] Excessively myofibroblasts produce excess matrix, distort the normal pulmonary structure, and result in progression of fibrosis. The activation of myofibroblasts is regulated by a variety of mechanisms, including paracrine signals derived from lymphocytes and macrophages[8] and autocrine factors secreted by myofibroblasts themselves.[9] Among these facts, the reactive oxygen species (ROS) is regarded as most important factor.[9,10]

ROS are involved in several cellular functions by triggering the proliferation, activation, hypertrophy and matrix accumulation.[11-13] It is demonstrated that increased ROS was required in the activation of myfibroblasts in lung fibrosis [9,14] and other fibrosis,[15,16] and served as target for anti-oxidant therapy to mitigate the fibrosis following IR.[17]

Though ROS play an essential role in myfibroblasts activation and fibrosis progression, the source of ROS in lung tissue is unverified.[18,19] It is believed that inflammatory cells are the main source of ROS. ROS could be produced by different inflammatory cells at different stages of disease and cross-act among the neutrophils, macrophages and fibroblast.[20]

The enzymes responsible for ROS generation are NOXes.[21] NOXes transfer electrons to oxygen, and then superoxide

**CONTACT** Chun Chen chenchun-0428@163.com; Lurong Zhang lurongzhang@ufl.edu
*These authors equally contributed to this work.

rapidly dismutates to ROS. NOX isoforms (NOX 1, NOX2 and NOX4) are involved in pulmonary fibrosis, obstructive lung disorders, and cystic fibrosis.[9,22-25] The NOXes knock down in animal models of fibrosis presented a marked reduced ROS and collagen production.[26,27] However, whether NOXes in macrophage contribute to oxidative stress in IR-induced pulmonary fibrosis remains to be elucidated.

TPL possesses anti-inflammation property. No study were conducted to explore effect of TPL on axis of AMs-NOXes-ROS-myofibroblasts, which is needed for the understanding of its molecular mechanism by which IR-induced lung fibrosis could be reduced by TPL

In this study, we found that AMs were the main inflammatory cells in IR-lung tissue, and NOXes dependent ROS from AMs induced myofibroblasts activation and collagen accumulation. TPL down-regulated NF$\kappa\beta$, NOX2 and NOX4 in AMs, and deprived the ROS-activated myofibroblasts and supressed IR-induced pulmonary fibrosis.

## Methods

### Animal model of thorax irradiation

C57BL/6 mice (female, 8 weeks old, National Cancer Institute, Frederic, MD, USA) were anesthetized by ketamine (80 mg/kg i.p.) and then placed in a special jig with 2 flaps to fix the head and ensure the lung was extended in radiation field in 3 splits collimator and irradiated with 15 Gy on whole thorax at a dose rate of 1.8Gy/min with Shepherd Mark-I irradiator.[28] The irradiated mice were then divided into groups (8 mice/group) for the different treatments: saline alone as vehicle control; TPL (0.25 mg/kg i.v 0.2 ml/mouse, q.o.d) for 1 months (dose and course of treatment were determined by previous study).[6] When the time came, the mice were euthanized and the right lungs were wire tied. Bronchoalveolar lavage fluids (BALF) were obtained just from left lungs. Following trachea intubation, the right lungs were perfused 5 times, each with 1 ml of PBS, and a total of >4 ml BAL fluid was retrieved. Thereafter, the right lungs were collected and divided into 3 pieces: one piece was fixed and embedded in paraffin for pathology and immunohistochemistry studies; another was used to prepare single cell suspensions; and the last piece was homogenized and stored at −80° C for cytokine analysis. All animal studies were approved by the institutional animal use committee and performed in accordance with National Institutes of Health (NIH) guidelines.

### Cell culture

Primary AMs were isolated from BALF obtained from every group, non-IR mice and thorax-IR mice. Cells from one group were pooled and adjusted to $1 \times 10^6$/ml, then plated in Dulbecco's modified Eagle medium (DMEM) containing 5% fetal bovine serum (FBS) as $2\tilde{}3 \times 10^5/cm^2$. Two hours later, non-attached cells were gently removed, and the medium was changed to Ultra-DOMA-PF (Lonza, Walkersville, MD, USA) without serum. Differential cell count was carried out on Wright-Giemsa-stained cytospin, smears, and the adherent AM population was >98%.

Mouse alveolar macrophage cell line MH-S was grown in RPMI 1640 containing 5% FBS and incubated for 24 h before exposure to radiation (Varian 600CD, Varian Medical Systems Inc., Palo Alto, CA, USA). After irradiation, cells were cultured for 24–72 h without a change of medium.

### Co-culture of AMs with fibroblasts

Two kinds of co-culture system were used: (1) co-culture of AMs with fibroblasts in Corning Transwell® plates (Sigma-Aldrich, St. Louis, MO, USA); (2) fibroblasts cultured with the conditioned AMs culture medium. In the first co-culture, AMs were cultured in Transwell inserts of a 12-well culture plate (0.4 $\mu$m pore size), and NIH3T3 cells (a mouse fibroblast cell line obtained from ATCC) were cultured in a 12-well plate. After the mediums of both AMs and fibroblasts were changed to 0.1% NCS DMEM for 1 day, the inserts containing AMs were then placed into the well containing NIH3T3 cells, and treated with saline or 300 $\mu$M apocynin (Sigma-Aldrich), an inhibitor of Noxes,[29] or TPL 5 ng/ml for 1 or 2 d. This co-culture system allowed the exchange of factors between 2 types of cells while there was no direct cell contact. For the medium transfer experiments in the 2nd co-culture, AMs and NIH3T3 were cultured separately for 1 day in which AMs were treated with or without 300 $\mu$M apocynin or TPL 5 ng/ml, and then the mediums of AMs were transferred to NIH3T3 wells and further cultured for 1 or 2 d.

### Flow Cytometry Analysis of AMs and myofibroblasts

Lungs were harvested at the indicated days from control and lung-IR mice with or without TPL treatment. One piece of lungs were minced and digested in DMEM medium containing 1 mg/ml collagenase (Sigma-Aldrich) for 45 min at 37°C. Any undigested fragments were further dispersed by drawing the solution up and down through the bore of a 5-ml syringe. Then, the cells were run through a 60-$\mu$m strainer and were washed and centrifuged. Cell counts and viability were determined using trypan blue exclusion on a hemocytometer. Single cell suspensions were stained with F4/80 combined with CD11b or anti-$\alpha$-SMA, followed by FITC-labeled or PE-labeled secondary antibodies. Samples were assayed immediately by Accuri C6 Flow Cytometer® and CFlow® software (BD Biosciences, Franklin Lakes, NJ, USA).

### Determination of ROS level

Levels of ROS in lung tissue were measured by flow cytometry. Briefly, the freshly harvested single cell suspensions from lung tissue (reflecting *in vivo* situation) were incubated with 25 $\mu$M 2,7-dichlorodihydrofluorescein diacetate (DCFH-DA, Sigma-Aldrich) for 25 min in dark, and then immediately analyzed with Accuri C6 Flow Cytometer®.

For the *in vitro* ROS production, the AMs from non-irradiated control mice and irradiated mice just receiving saline for 1 month were pooled respectively, cultured in 96 well plates and treated with or without Noxes inhibitor-Apocynin (Apo, 300 $\mu$M) or TPL (5 ng/ml) (n = 5, in duplicate) for 6 or 12 hr, and then incubated with 25 $\mu$M of DCFH-DA for 25 min in

dark. The fluorescence was read immediately at 485 nm for excitation and 530 nm for emission with a Spectramax (Sunnyvale, CA, USA).

The ROS values were expressed as fold changes compared to the controls.

### Western blot analysis

Cell lysates (30 $\mu$g/lane) were separated by 10% SDS-polyacrylamide gel electrophoresis and electrotransferred onto polyvinylidene fluoride (PVDF) membranes (EMD Millipore Corporation, Billerica, MA, USA). After blocked with 5% nonfat milk, membranes were probed with primary antibodies (anti-NOX1, anti-NOX2/gp91phox, anti-NOX4, anti-$\alpha$-smooth muscle actin (anti-$\alpha$-SMA), anti-NF$\kappa$B(p65), anti-I$\kappa$B$\alpha$, anti-Lamin B, and anti-$\beta$-actin (Abcam, Cambridge, MA, USA) followed by peroxidase-labeled secondary antibody, and visualized with Pierce ECL Western Blotting Substrate (Thermo Fisher Scientific Inc., Rockford, IL, USA). The density of NOXes was scanned and analyzed, and the values were expressed as the relative expression of protein normalized to $\beta$-actin protein.

### siRNA Inhibition of NOX2 and NOX4

MH-S cells were grown to50%–60% confluence in RPMI 1640 containing 10% fetal bovine serum without antibiotic, and then transfected with nontargeting Control siRNA, si-m-Cybb (NOX2) or si-m-NOX4 (RiboBio Co., Ltd., Guangzhou, China) using X-tremeGene siRNA transfection reagent (Roche Diagnostics Corp., Indianapolis, IN) according to the manufacturers' instructions. The final optimized concentration for siRNAs was 20 nM. The transfection rate was about 80% – 85% as confirmed by transfecting with nontargeting Control siRNA (cy3) and detecting the fluorescence using Cellomics Arrayscan VT1 (Thermo Scientific, MA, USA). For Western blotting analysis, the cells were allowed to grow for an additional 48 h. One of 3 siRNAs duplexes, siNOX2 (duplex1) and siNOX4( duplex 1), efficiently blocked NOX2 or NOX4 expression. Transfected MH-S cells were raised up in RPMI 1640 containing 10% fetal bovine serum without antibiotic.

### Staining for AMs or myofibroblasts

AMs or myofibroblasts in lungs were stained using their specific cell-surface marker F4/80 (anti-active macrophage) or anti-$\alpha$-SMA with standard immunohistochemical staining.[2] In brief, Lung tissue sections were routinely rehydrated, antigen retrieved by using microwave and incubated in hydrogen peroxide for 10 min. After wash with PBS, sections were incubated with primary antibody for F4/80 and $\alpha$-SMA (Santa Cruz Biotechnology) for 2 h. Following extensive washing, sections were incubated for 30 min in the secondary HRP-conjugated antibody followed by AEC kit. Sections were then counter-stained with hematoxylin. Images were captured by using Zeiss microscope (Zeiss Axioplan 2 Imaging, Oberkochen, Germany).

NIH3T3 cells were grown on glass coverslips and co-culture with different conditioned medium of AMs for 1 day which detailed in "Co-culture of AMs with fibroblasts." Then the cells fixed in ice-cold acetone for 10 min, incubated with 1% BSA in PBST for 30 min to block unspecific binding. After incubated with primary antibody for 1 h at room temperature, cells were incubated with FITC conjugated secondary antibody (BD Biosciences, San Jose, CA 95131) for 30 min at dark. Cells were counter stained with DAPI and images were captured under Zeiss microscope.

### Collagen stained with Masson's Trichrome blue or quantitated with Picro-Sirius red assay

Trichrome blue was used to stain collagens in lung tissue sections.[2] In brief, lung tissue sections were routinely rehydrated, antigen retrieved and incubated in hydrogen peroxide for 10 min. After wash with PBS, sections were stained by trichrome stain.

To quantitate the collagen in cell culture supernatants and lung homogenates, the Picro-Sirius red staining method was used as previously described.[28]

### Statistical analysis

Quantitative data were expressed as mean and standard deviation. Statistical analysis of the data was performed with ANOVA and *t*-test. Differences with $p$ values $<0.05$ were considered to be statistically significant.

## Results

### Mitigation of radiation induced pulmonary fibrosis by TPL was associated with reduced myofibroblasts and ROS

IR is a strong inducer of pulmonary fibrosis. The induction is a relatively slow process. At the early stage, there was no significant collagen deposition. One month after the IR, the collagen deposition (Figs. 1A and B) moderately increased and lung septal thickening was observed. Meanwhile, an up-regulated $\alpha$-SMA expression in IR-lung tissues was detected by both flow cytometry and immunohistochemistry staining (Figs. 1C and D), which indicates excessive myofibroblasts activation. Accompanied with increased myofibroblasts activation, a marked increase of ROS (up to 5.5 times) was detected in lung tissue (Fig. 1E), and TPL treatment significantly reduced the activation of myofibroblasts and the level of ROS in irradiated lung tissues. By the fifth month post the IR, the lung damage became very obviously (Fig. 1F). The number of alveoli dramatically decreased, even disappeared in some areas. The collagen deposition increased about 200% (Fig. 1G). The treatment with TPL significantly reduced the lung damage induced by the IR. The alleviation of IR induced pulmonary fibrosis by TPL (0.25 mg/kg for 1 month) was found as early as one month post the IR and it was much significant in the 5th month after 15 Gy thorax ionizing radiation, as evidenced by reduced lung collagen deposition on histochemical staining (Fig. 1F) and collagen quantification (Fig. 1G). This effect is much better than Amifostine, a cytoprotective adjuvant that could be used for reducing side effects during chemotherapy and radiation treatment.

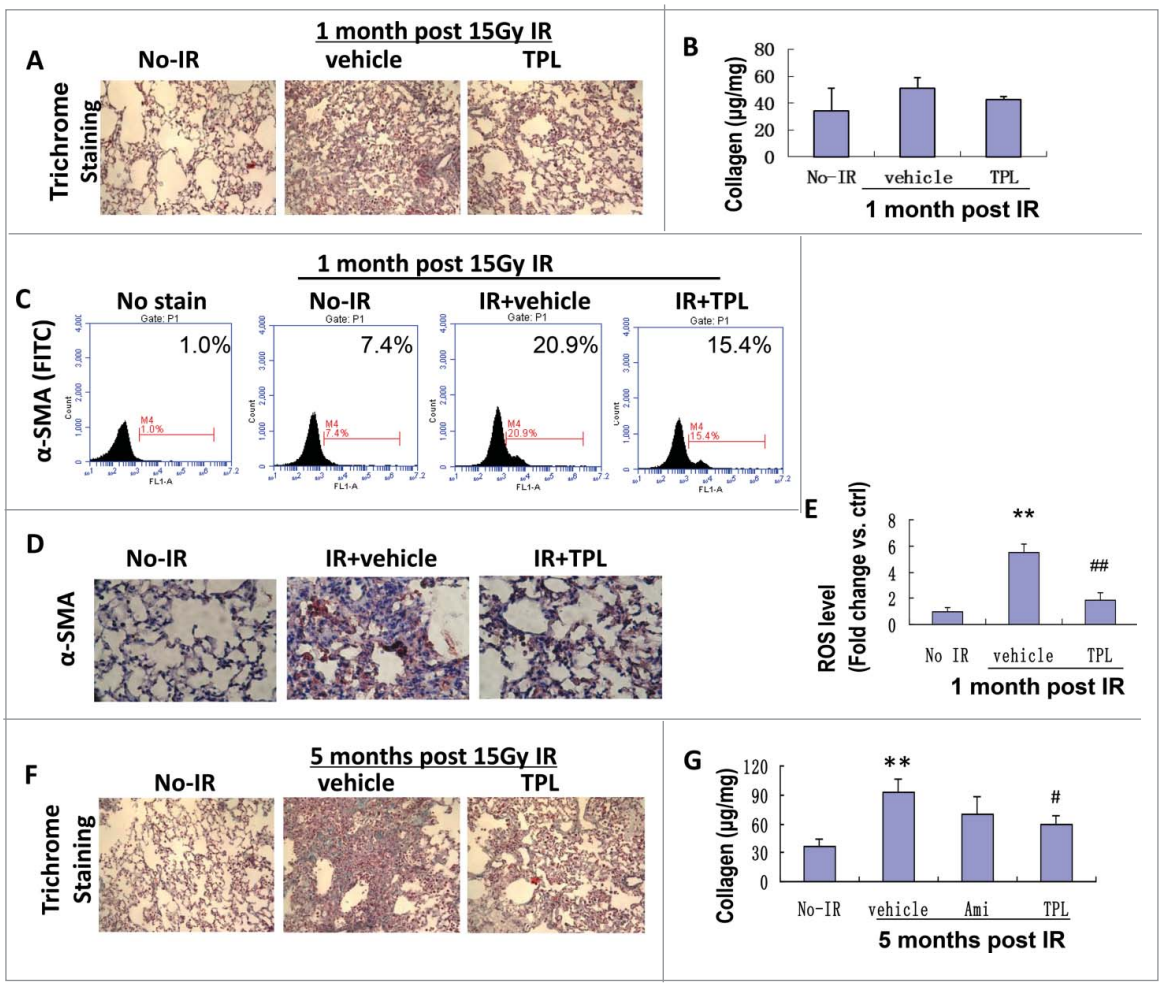


**Figure 1.** TPL mitigated IR-induced lung fibrosis via reduction of myofibroblasts and ROS Levels. (A) One month post IR impaired tissue structure but little collagen deposition were visualized by Trichrome staining (×100). (B) Collagen level in lung tissue was determined by Sirius red method using lung homogenate. Myofibroblasts characterized by α-SMA expression was detected by flow cytometry (C) and immunohistochemistry (D, ×200). (E) ROS level in lung tissue was measured by flow cytometry as the fluorescence of DCF. (F) Lung fibrosis formed 5 month post 15 Gy thorax IR and collagen deposition were visualized by Trichrome staining (×100). (G) Collagen levels in lung homogenate were determined by Sirius red assay (n = 5). Ami: Amifostin 200 mg/kg for 1 month, TPL: TPL 0.25 mg/kg for 1 month. $^{**}P < 0.01$, IR vehicle ctrl vs no-IR; #P < 0.05, ## P < 0.01, TPL vs. IR vehicle.

### *Increased ROS was released from AMs upon IR exposure*

According to the essential role of ROS in myfibroblasts activation and fibrosis progression, we explored the source of increased ROS in irradiated lung tissue. ROS is secreted by varied cell types, and myofibroblasts themselves are reported as a source of ROS. Our results showed that in irradiated lung tissue at early stage, myofibroblasts were just moderately increased, but ROS level reached to 5.5 times higher than in no IR lung tissue. A large proportion of ROS should come from cells other than myofibroblasts. Inflammatory cells are the main source of ROS. The cellular components in the BALF varied with time after IR: on day 2.5, the lymphocytes and AMs dominated with few neutrophils; on day 17, the neutrophils, AMs, and dead epithelial cells were dominant (data not shown); 1 month after IR, AMs accounted for more than 85% of total infiltrated cells (Table 1) with a 2-fold increase in the cell number. Immunohistochemical and flow cytometry results also showed a significant increase of AMs in irradiated lung tissue (Figs. 2A and B). These demonstrated that AMs were the dominant inflammatory cells after the irradiation.

To confirm that the high level of ROS in IR-lungs was related to macrophages, AMs were isolated from control (AMs-ctrl) and thorax irradiated mice (AMs-IR), and their intracellular ROS level was studied at different time points (6 hr and 12 hr). Results (Fig. 2C) showed that significantly increased ROS production (2.7 fold) was observed in AMs-IR compared to AMs-Ctrl, which was inhibited by TPL..

**Table 1.** Total and differential cells counted at BALF 1 month post lung-IR.

| Subjects | Total cell $ml^{-1}$ BAL | AMs (%) | Lympho (%) | PMNs (%) |
|---|---|---|---|---|
| control(n=8) | $2.6 \times 10^4$ | 89.2 ± 1.2 | 8.2 ± 1.4 | 2 ± 1 |
| lung-IR(n=7) | $6.8 \times 10^{4*}$ | 85.7 ± 2 | 10.4 ± 3 | 3.4 ± 0.5 |
| IR+TPL(n=8) | $3.9 \times 10^{4\dagger}$ | 89.6 ± 1.4 | 7.6 ± 2.2 | 2.2 ± 0.5 |

View it in a separate window

Data were expressed as total cell number $ml^{-1}$ of BAL and percentage of total cell population (differential) in BAL. AMs=alveolar macrophages; Lympho=alveolar lymphocytes; PMNs=alveolar neutrophils. * Denotes P < 0.01 vs. control, † Denotes P < 0.01 vs. lung-IR.

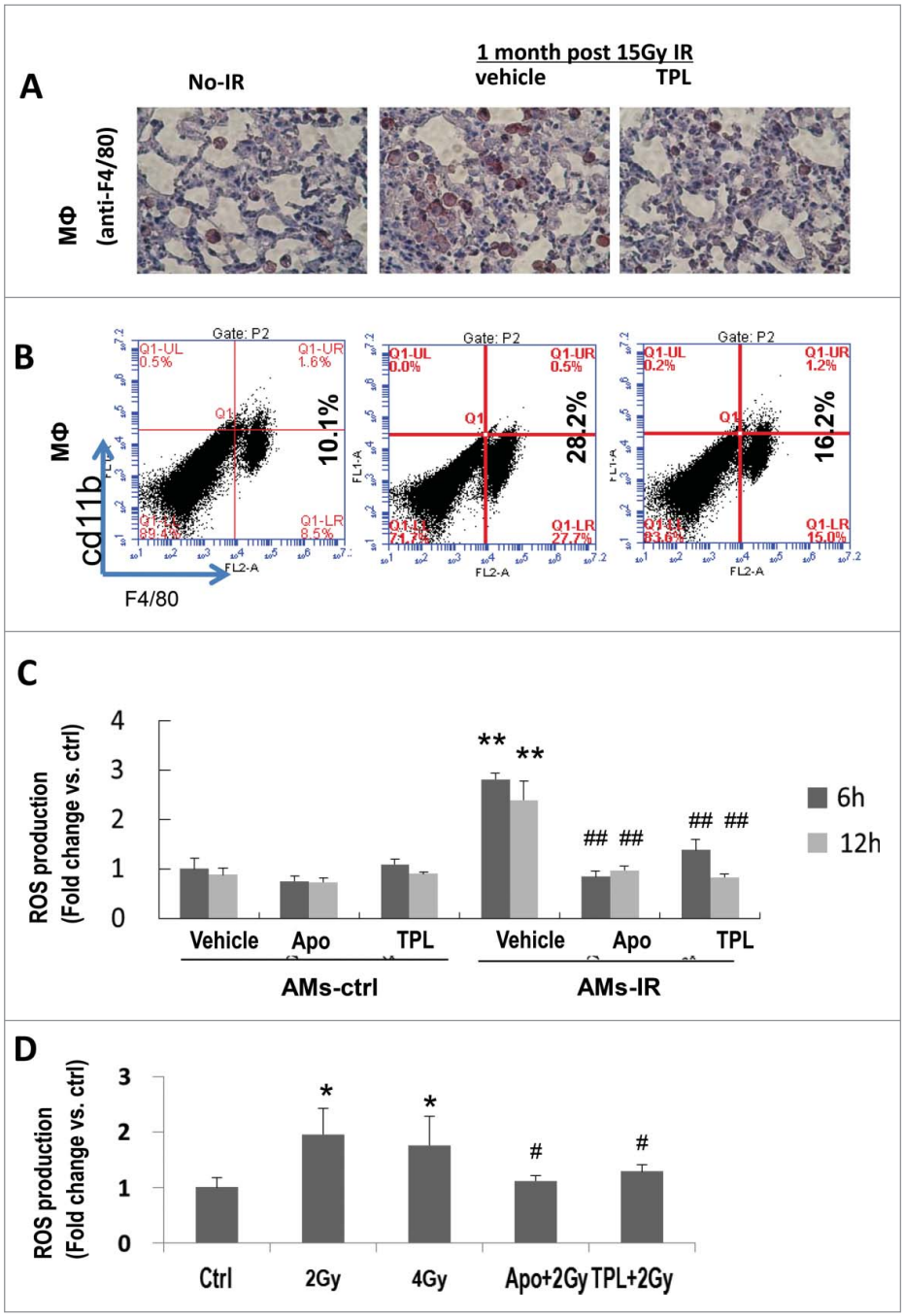


**Figure 2.** TPL reduced the infiltrated AMs and inhibited the production of ROS from AMs-IR. (A) Macrophage in lung tissue was detected by immunohistochemistry (×400) and Flow cytometry (B). (C) Cultured AMs-ctrl and AMs-IR were treated with or without Apocynin (Apo, 300 $\mu$M) or TPL (5 ng/ml) (n = 5, in duplicate) for 6 h and 12 h, and ROS production was measured by DCFH-DA fluorescence assay. Values are expressed as mean ± sd, relative to Ctrl. $^{**}$P< 0.01 vs. ctrl vehicle; ##P < 0.01 vs. IR vehicle. (D) ROS production was measured in irradiated MH-S cells with or without pretreated by Apocynin or TPL for 4 h. $^{*}$ P < 0.05 vs. Ctrl; # P < 0.05 vs. 2 Gy.

To further confirm that IR stimulates AMs producing more ROS, a mouse alveolar macrophage cell line MH-S was used. Indeed, IR triggered MH-S cells producing more ROS than control cells did, which was also inhibited by TPL (Fig. 2D). There was no difference between the irradiated with 2 Gy or 4 Gy, suggesting that the 2 Gy is sufficient for triggering ROS production in MH-S cells.

Taken together, both *in vivo* and *in vitro* data indicate that upon IR, AMs were the main source of ROS.

### *ROS originated from AMs induced myofibroblasts activation*

To evaluate the paracrine effect of ROS produced by AMs on fibroblast/myofibroblasts activation and collagen accumulation, 2 systems for macrophage/fibroblast interaction were used.

First, the AM conditioned medium (CM) was transferred to the cultured NIH 3T3 fibroblasts for 1 or 2 d Results (Fig. 3A lane 5 and 3C set 4) showed that the AMs-IR CM induced

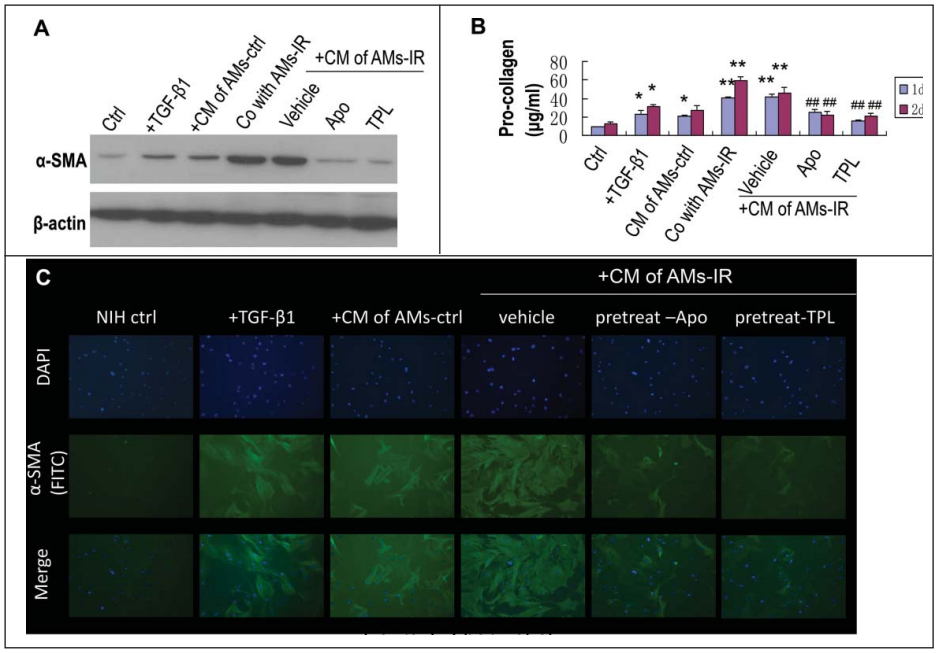


**Figure 3.** TPL and Apocynin abrogated AMs-IR induced myofibroblast activation and pro-collagen secretion. NIH3T3 cultured with conditioned medium (CM) of AMs for 1 or 2days, or NIH3T3 co-cultured with AMs-IR using transwell for 1 or 2days. (A) The level of $\alpha$-SMA in myofibroblasts was measured by Western blot. (B) The level of pro-collagen in CM was assayed by Sirus red method (n = 3). (C) NIH3T3 cells were grown on glass coverslips and cultured with CM for 2days, and then the $\alpha$-SMA expression in myofibroblasts was detected by immunofluorescent staining($\times$ 400). +**TGF-$\beta$1**: NIH3T3 treated with TGF-$\beta$1 (5 ng/ml); + **CM of AMs-ctrl**: AMs-ctrl culture alone for 1day, then the CM of AMs-ctrl was transferred to the culture well of NIH3T3; + **CM of AMs-IR (vehicle, Apo or TPL)**: AMs-IR treated without (vehicle) or with Apocynin (Apo, 300 mM) or TPL (5ng/ml) for 1day, then the CM was transferred to the culture well of NIH3T3; **Co with AMs-IR**: transwell® co-culture of AMs-IR with NIH3T3. AMs-IR were cultured in transwell inserts (0.4 $\mu$m pore size), and NIH3T3 cells were cultured in the bottom of transwell plate. ** $P < 0.01$ vs. ctrl; ## $P < 0.01$ vs. CM of AMs-IR (vehicle).

significantly increased the levels of $\alpha$-SMA and procollagen secretion in fibroblasts (Fig. 3B lane 5) while the AMs-ctrl CM did not possess such an effect (Fig. 3A lane 3, Fig. 3C set 3 and Fig. 3B lane 3).

Second, a transwell (0.4 $\mu$m pore size) co-culture system was used (AMs-IR on the top and NIH 3T3 fibroblasts on the bottom of the well). This allowed the exchange of factors between 2 types of cells without direct cellular contact. The $\alpha$-SMA level and the procollagen secretion were increased in fibroblasts (Fig. 3A lane 4 and 3B lane 4).

Taken together, ROS from AMs-IR played an essential role in IR-induced pulmonary fibrosis by promoting myofibroblasts activation and collagen accumulation.

### *Radiation-increased ROS in AMs was NOX2 and NOX4 dependent*

To prove that IR-increased ROS in AMs was NOX2 and NOX4 dependent, Apocynin (a broad NOX inhibitor[29,30]) was used. When cultured AMs-IR were treated with Apocynin, the ROS elevation was abrogated. Same results were obtained from irradiated MH-S cells pretreated with Apocynin (Fig. 2D), suggesting that NOXes were involved in the IR-induced production of ROS in AMs. In addition, Apocynin also significantly inhibited AMs-IR induced $\alpha$-SMA expression and procollagen accumulation, implicating that NOXes derived ROS in AMs-IR CM promotes the myofibroblast activation, resulting in excessive procollagen production.

There are several isoforms in the NOX family.[25,31] Among these, NOX1, NOX2 and NOX4 have been reported to contribute in tissue fibrosis.[25] Using Western blotting, we found NOX-1, NOX2 and NOX4 were all expressed in AMs (Fig. 4A). NOX2 and NOX4 were upregulated by IR in AMs-IR as compare to AMs-Ctrl (Figs. 4A and B). The expression level was correlated with enhanced ROS production (Fig. 2C). The level of NOX-1 had no significant change among the AMs, AMs-TPL, AMs-IR-Ctrl and AMs-IR-TPL, suggesting that NOX-1 might not play a key role in IR-triggered NOX-ROS production.

Increased levels of NOX2 and NOX4 were also detected in irradiated MH-S cells (Fig. 4C). To further define the role of NOX2/NOX4 in ROS production and fibroblast transforming into myofibroblast, small interference RNA (siRNA) knockdown experiments were carried out. Western blotting (Fig. 4D) showed that NOX2 and NOX4 protein were significantly decreased by transfection with siNOX2 and siNOX4. Meanwhile, the productions of IR-induced ROS in the siNOX2 and siNOX4 downregulated cells were also reduced with a more striking effect in siNOX2 cells (Fig. 4E). The data indicates that the NOX2 and NOX4 are major players in IR-triggered ROS production, especially the NOX2, which in turn, leads to myofibroblasts activation.

### *TPL mitigated the profibrotic effect of AMs-IR partly by down-regulating NOX2 through NF$\kappa$B pathway*

Since TPL is a well-known NF$\kappa$B depressor,[32] we wanted to explore if IR-induced activation of I$\kappa$B$\alpha$ could be affected by TPL and if IKK$\beta$ inhibitors TPCA-1[33] had a similar effect as TPL on NOX2.

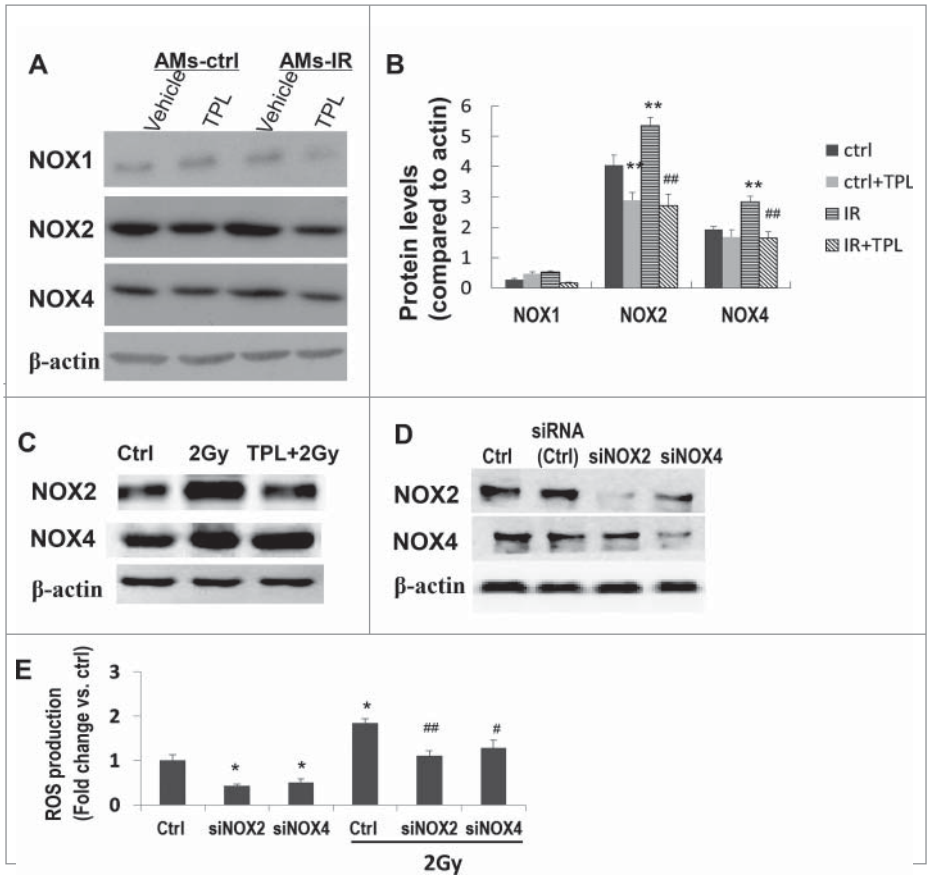


**Figure 4.** Increased ROS secretion by irradiated AMs were NOX2 and NOX4 dependent. (A) AMs-ctrl and AMs-IR were treated with or without TPL (5 ng/ml) (n = 3–4 independent experiments), and the protein level of NOXes was measured by Western blot and normalized to $\beta$-actin protein levels (B). ** P < 0.01 vs. ctrl; ## P < 0.01 vs. IR. (C) NOXes in irradiated MH-S cells with or without TPL treatment. (D) Knock down NOX2 or NOX4 in MH-S cells by siNOX2 or siNOX4. (E) ROS production by MH-S cells with or without NOX2 or NOX4 silence. * P < 0.05 vs. Ctrl; # P < 0.05, ##P < 0.01 vs. 2 Gy Ctrl.

Upon 2 Gy irradiation, the I$\kappa$B$\alpha$ was phosphorylated in cytoplasma of MH-S cells and the nucleus translocation of NF$\kappa$B was enhanced (Fig. 5A). IKK$\beta$ inhibitors TPCA-1reduced both NOX expression and ROS generation in irradiated MH-S cells (Figs. 5B and C). These results suggested that IR up-regulated NF$\kappa$B pathway in alveolar macrophages, and then partially control the NOX2 expression and ROS production. TPL significantly decreased the cytoplasmic level of pI$\kappa$B$\alpha$ and nuclear level of NF$\kappa$B (p65), which could, in turn, reduced the NOX expression and ROS generation as TPCA-1 did.

## Discussion

In this study, we demonstrated for the first time that TPL mitigates IR-induced pulmonary fibrosis via inhibition of axis of NOXes-ROS in AMs and its effect on myofibroblast transformation as well as collagen production.

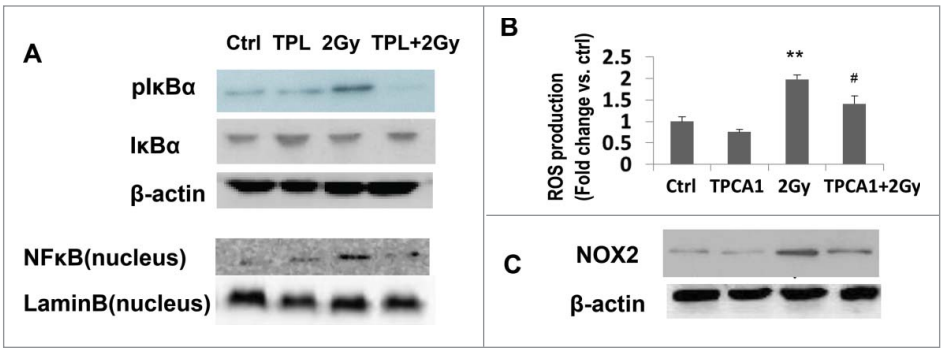


**Figure 5.** NF$\kappa$B pathway involved in NOX2 regultion and ROS production in irradiated MH-S cells. (A) The protein level of pI$\kappa$B$\alpha$ and nuclear NF$\kappa$B in MH-S cells treated by IR or TPL or both. (B) IKK$\beta$ inhibitor TPCA-1 regulated ROS generation and NOX2 expression (C) in irradiated MH-S cells. **P< 0.01 vs. Ctrl; # P < 0.05 vs. 2 Gy.

The key role of AMs in the progression of IR-induced lung damage is evidenced by the following factors: (**1**) after IR, the dominated infiltrated cells were shift from neutrophils /lymphocytes to AMs, which peaked at one month and lasted for several months. The evidence suggests that AMs are related in the progression of IR-induced pulmonary fibrosis; (2) Although the source of ROS in lung comes from a variety of cell types, such as leukocytes,[18] epithelial cells [19] and myofibroblasts,[9] the AMs are the main sources of ROS in IR lung tissue. Radiation not only induced AMs infiltration but also enhanced ROS secretion by AMs, leading to greatly increased ROS in lung tissue; (3) The results of either transferring the culture media of AMs to fibroblasts or transwell co-culture of AMs with fibroblasts suggest that via paracrine and ROS effects, AMs are capable to activate myofibroblasts and promote the production of collagen. Our data is consistent with other's reports that AMs had multiple functions in the initiation and promotion of pulmonary fibrosis,[34-36] including regulating inflammatory cells, recruiting and activating myofibroblasts, and producing and secreting pro-inflammation cytokines and chemokines.[12,34-36] The selective depletion of macrophages could result in a significant reduction in bleomycin-induced pulmonary fibrosis.[37] However, these previous reports did not reveal the interactions among the alveolar macrophages, NOXes, ROS and myofibroblasts. Importantly, the response of AMs to IR could be elicited at the clinically relevant dose of 2 Gy and occurred as early as being irradiated, especially for the generation of ROS.

Using NOXes inhibitor, Apocynin, and siRNA knockdown technique, we also demonstrated that NOX2 and NOX4, but not NOX1, were responsible for IR- increased ROS production in AMs, which further affected the myofibroblasts.

We also proved that at the clinically relevant 2 Gy IR dose, NF$\kappa$B pathway could be activated as evidenced by the phosphorylated I$\kappa$B$\alpha$ and increased nucleus NF$\kappa$B. The IKK$\beta$ inhibitor TPCA-1 could act like TPL to inhibit the NOX2 and ROS production, but partially, suggesting that there should be other pathway involved in regulation of NOX2 and NOX4.

Importantly, we revealed that the anti-IR lung fibrosis effect of TPL (Figs. 1A–D ) was related with its inhibition of the functions of 2 critical types of profibrosis cells: the AMs (Figs. 2A and B) and transformed myofibroblasts (Fig. 1E and F, Fig 3) by interference of following key molecules: (1) suppressing the IR-activated NF$\kappa$B pathway (Fig 5A); (2) reducing the IR-triggered expression of NOXes (Figs. 4A-C) and ROS (Figs. 1G, 2C–D). Our new findings define the IR-induced pro-fibrotic axis of AMs-NOXes-ROS-myofibroblasts, and reveal the TPL suppression of this axis to alleviate the process of IR-lung fibrosis.

IR-induced pulmonary injuries can be divided into 2 phases: acute inflammation (about 1 month) and chronic fibrosis (a few months to years). We previously reported that lung irradiated C57BL/6 mice treated with TPL for only 1 month exhibited significant mitigation effect on pulmonary fibrosis.[6] By adjusting the pathophysiological changes in the early inflammation stages, TPL inhibited the progression of lung fibrosis in later stages via suppressing the profibrotic effect of AMs-IR.

Taken together, our results showed that NOX-dependent ROS in AMs-IR mediates myofibroblast activation. TPL blocks the paracrine activation of myofibroblasts and reduced collagen production through its inhibition of NOX-related ROS in AMs-IR, which could be utilized for anti-IR induced lung damage therapy.

## Disclosure of potential conflicts of interest

No potential conflicts of interest were disclosed.

## Funding

This study is supported in part by grant supports from the Scientific Research Foundation for the Returned Overseas Chinese Scholars, State Education Ministry (2013B025) and Fujian provincial natural science fund (2014J01336) to CC; NIH (NIAID: RC2-AI-087580, RC1-AI-078519 and RC1-AI-081274) to LZ and SY, We thank Kate Casey-Sawicki for her professionally editing this manuscript.

## Summary

Ionizing radiation (IR)-induced pulmonary fibrosis is a severe complication of radiotherapy for the patients with lung cancer. Triptolide (TPL), a diterpenoid epoxide purified from *Tripterygium wilfordii*, possesses dual effect of both anti-cancer and anti-inflammation. In this study, we revealed its mechanism of anti-IR-induced lung fibrosis via inhibition of axis of alveolar macrophages-NOXes-ROS-myofibroblasts.

## References

1. Dicarlo AL, Jackson IL, Shah JR, Czarniecki CW, Maidment BW, Williams JP. Development and licensure of medical countermeasures to treat lung damage resulting from a radiological or nuclear incident. Radiat Res 2012; 177:717-721; PMID:22468704; http://dx.doi.org/10.1667/RR2881.1
2. Krishna G, Liu K, Shigemitsu H, Gao M, Raffin TA, Rosen GD. PG490-88, a derivative of triptolide, blocks bleomycin-induced lung fibrosis. Am J Pathol 2001; 158:997-1004; PMID:11238047; http://dx.doi.org/10.1016/S0002-9440(10)64046-1
3. Ren YX, Zhou R, Tang W, Wang WH, Li YC, Yang YF, Zuo JP. (5R)-5-hydroxytriptolide (LLDT-8) protects against bleomycin-induced lung fibrosis in mice. Acta Pharmacol Sin 2007; 28:518-525; PMID:17376291; http://dx.doi.org/10.1111/j.1745-7254.2007.00524.x
4. Chong LW, Hsu YC, Chiu YT, Yang KC, Huang YT. Antifibrotic effects of triptolide on hepatic stellate cells and dimethylnitrosamine-intoxicated rats. Phytother Res 2011; 25:990-999; PMID:21213358; http://dx.doi.org/10.1002/ptr.3381
5. Yuan XP, He XS, Wang CX, Liu LS, Fu Q. Triptolide attenuates renal interstitial fibrosis in rats with unilateral ureteral obstruction. Nephrology (Carlton) 2011; 16:200-210.
6. Yang Shanmin ZM, Cao Y, Chen C, Tian Y, Zhang B, Wang X, Guo Y, Zhang L, Okunieff P. Triptolide mitigates radiation-induced pulmonary fibrosis and its action mechanism(Conference abstract). I J Radiat Oncol Biol Phys 2011; 81:S194-S195.
7. Abraham DJ, Eckes B, Rajkumar V, Krieg T. New developments in fibroblast and myofibroblast biology: implications for fibrosis and scleroderma. Curr Rheumatol Rep 2007; 9:136-143; PMID:17502044; http://dx.doi.org/10.1007/s11926-007-0008-z
8. Rubin P, Finkelstein J, Shapiro D. Molecular biology mechanisms in the radiation induction of pulmonary injury syndromes: interrelationship between the alveolar macrophage and the septal fibroblast. Int J Radiat Oncol Biol Phys 1992; 24:93-101; PMID:1512168; http://dx.doi.org/10.1016/0360-3016(92)91027-K
9. Hecker L, Vittal R, Jones T, Jagirdar R, Luckhardt TR, Horowitz JC, Pennathur S, Martinez FJ, Thannickal VJ. NADPH oxidase-4

mediates myofibroblast activation and fibrogenic responses to lung injury. Nat Med 2009; 15:1077-1081; PMID:19701206; http://dx.doi.org/10.1038/nm.2005
10. Barnes JL, Gorin Y. Myofibroblast differentiation during fibrosis: role of NAD(P)H oxidases. Kidney Int 2011; 79:944-956; PMID:21307839; http://dx.doi.org/10.1038/ki.2010.516
11. Kamata H, Honda S, Maeda S, Chang L, Hirata H, Karin M. Reactive oxygen species promote TNFalpha-induced death and sustained JNK activation by inhibiting MAP kinase phosphatases. Cell 2005; 120:649-661; PMID:15766528; http://dx.doi.org/10.1016/j.cell.2004.12.041
12. Yarnold J, Brotons MC. Pathogenetic mechanisms in radiation fibrosis. Radiother Oncol 2010; 97:149-161; PMID:20888056; http://dx.doi.org/10.1016/j.radonc.2010.09.002
13. Zou CG, Gao SY, Zhao YS, Li SD, Cao XZ, Zhang Y, Zhang KQ. Homocysteine enhances cell proliferation in hepatic myofibroblastic stellate cells. J Mol Med (Berl) 2009; 87:75-84; PMID:18825355; http://dx.doi.org/10.1007/s00109-008-0407-2
14. Bocchino M, Agnese S, Fagone E, Svegliati S, Grieco D, Vancheri C, Gabrielli A, Sanduzzi A, Avvedimento EV. Reactive oxygen species are required for maintenance and differentiation of primary lung fibroblasts in idiopathic pulmonary fibrosis. PLoS One 2010; 5:e14003; PMID:21103368; http://dx.doi.org/10.1371/journal.pone.0014003
15. Bondi CD, Manickam N, Lee DY, Block K, Gorin Y, Abboud HE, Barnes JL. NAD(P)H oxidase mediates TGF-beta1-induced activation of kidney myofibroblasts. J Am Soc Nephrol 2010; 21:93-102; PMID:19926889; http://dx.doi.org/10.1681/ASN.2009020146
16. Lan T, Kisseleva T, Brenner DA. Deficiency of NOX1 or NOX4 Prevents Liver Inflammation and Fibrosis in Mice through Inhibition of Hepatic Stellate Cell Activation. PLoS One 2015; 10:e0129743; http://dx.doi.org/10.1371/journal.pone.0129743. eCollection 2015
17. Jackson IL, Chen L, Batinic-Haberle I, Vujaskovic Z. Superoxide dismutase mimetic reduces hypoxia-induced $O2^{*}$-, TGF-beta, and VEGF production by macrophages. Free Radic Res 2007; 41:8-14; PMID:17164174; http://dx.doi.org/10.1080/10715760600913150
18. Macnee W. Oxidants/antioxidants and COPD. Chest 2000; 117:303S-317S; PMID:10843965; http://dx.doi.org/10.1378/chest.117.5_suppl_1.303S-a
19. Babbar N, Casero RA, Jr. Tumor necrosis factor-alpha increases reactive oxygen species by inducing spermine oxidase in human lung epithelial cells: a potential mechanism for inflammation-induced carcinogenesis. Cancer Res 2006; 66:11125-11130; PMID:17145855; http://dx.doi.org/10.1158/0008-5472.CAN-06-3174
20. Tsoutsou PG, Koukourakis MI. Radiation pneumonitis and fibrosis: mechanisms underlying its pathogenesis and implications for future research. Int J Radiat Oncol Biol Phys 2006; 66:1281-1293; PMID:17126203; http://dx.doi.org/10.1016/j.ijrobp.2006.08.058
21. Forman HJ, Torres M. Reactive oxygen species and cell signaling: respiratory burst in macrophage signaling. Am J Respir Crit Care Med 2002; 166:S4-8; PMID:12471082; http://dx.doi.org/10.1164/rccm.2206007
22. Griffith B, Pendyala S, Hecker L, Lee PJ, Natarajan V, Thannickal VJ. NOX enzymes and pulmonary disease. Antioxid Redox Signal 2009; 11:2505-2516; PMID:19331546; http://dx.doi.org/10.1089/ars.2009.2599
23. Carnesecchi S, Deffert C, Donati Y, Basset O, Hinz B, Preynat-Seauve O, Guichard C, Arbiser JL, Banfi B, Pache JC, Barazzone-Argiroffo C, Krause KH. A key role for NOX4 in epithelial cell death during development of lung fibrosis. Antioxid Redox Signal 2011; 15:607-619; PMID:21391892; http://dx.doi.org/10.1089/ars.2010.3829
24. Zhang X, Shan P, Jiang G, Cohn L, Lee PJ. Toll-like receptor 4 deficiency causes pulmonary emphysema. J Clin Invest 2006; 116:3050-3059; PMID:17053835; http://dx.doi.org/10.1172/JCI28139
25. Hecker L, Cheng J, Thannickal VJ. Targeting NOX enzymes in pulmonary fibrosis. Cell Mol Life Sci 2012; 69:2365-2371; PMID:22618245; http://dx.doi.org/10.1007/s00018-012-1012-7
26. Wang H, Chen X, Su Y, Paueksakon P, Hu W, Zhang MZ, Harris RC, Blackwell TS, Zent R, Pozzi A. p47(phox) contributes to albuminuria and kidney fibrosis in mice. Kidney Int 2015; 87:948-962; PMID:25565313; http://dx.doi.org/10.1038/ki.2014.386
27. Hecker L, Logsdon NJ, Kurundkar D, Kurundkar A, Bernard K, Hock T, Meldrum E, Sanders YY, Thannickal VJ. Reversal of persistent fibrosis in aging by targeting Nox4-Nrf2 redox imbalance. Sci Transl Med 2014; 6:231ra247; http://dx.doi.org/10.1126/scitranslmed.3008182
28. Chen C, Yang S, Zhang M, Zhang Z, Zhang B, Han D, Ma J, Wang X, Hong J, Guo Y, Okunieff P, Zhang L. In vitro sirius red collagen assay measures the pattern shift from soluble to deposited collagen. Adv Exp Med Biol 2013; 765:47-53; PMID:22879013; http://dx.doi.org/10.1007/978-1-4614-4989-8_7
29. Bedard K, Krause KH. The NOX family of ROS-generating NADPH oxidases: physiology and pathophysiology. Physiol Rev 2007; 87:245-313; PMID:17237347; http://dx.doi.org/10.1152/physrev.00044.2005
30. Lemarie A, Bourdonnay E, Morzadec C, Fardel O, Vernhet L. Inorganic arsenic activates reduced NADPH oxidase in human primary macrophages through a Rho kinase/p38 kinase pathway. J Immunol 2008; 180:6010-6017; PMID:18424721; http://dx.doi.org/10.4049/jimmunol.180.9.6010
31. Yeligar SM, Harris FL, Hart CM, Brown LA. Ethanol induces oxidative stress in alveolar macrophages via upregulation of NADPH oxidases. J Immunol 2012; 188:3648-3657; PMID:22412195; http://dx.doi.org/10.4049/jimmunol.1101278
32. Wang X, Zhang L, Duan W, Liu B, Gong P, Ding Y, Wu X. Anti-inflammatory effects of triptolide by inhibiting the NF-kappaB signalling pathway in LPS-induced acute lung injury in a murine model. Mol Med Rep 2014; 10:447-452; PMID:24789089; http://dx.doi.org/10.3892/mmr.2014.2191. Epub 2014 Apr 28.
33. Podolin PL, Callahan JF, Bolognese BJ, Li YH, Carlson K, Davis TG, Mellor GW, Evans C, Roshak AK. Attenuation of murine collagen-induced arthritis by a novel, potent, selective small molecule inhibitor of IkappaB Kinase 2, TPCA-1 (2-[(aminocarbonyl)amino]-5-(4-fluorophenyl)-3-thiophenecarboxamide), occurs via reduction of proinflammatory cytokines and antigen-induced T cell Proliferation. J Pharmacol Exp Ther 2005; 312:373-381; http://dx.doi.org/10.1124/jpet.104.074484
34. Koh TJ, Dipietro LA. Inflammation and wound healing: the role of the macrophage. Expert Rev Mol Med 2011; 13:e23; PMID:21740602; http:dx.doi.org/10.1017/S1462399411001943
35. Danenberg HD, Fishbein I, Gao J, Monkkonen J, Reich R, Gati I, Moerman E, Golomb G. Macrophage depletion by clodronate-containing liposomes reduces neointimal formation after balloon injury in rats and rabbits. Circulation 2002; 106:599-605; PMID:12147543; http://dx.doi.org/10.1161/01.CIR.0000023532.98469.48
36. Zhang-Hoover J, Sutton A, Van Rooijen N, Stein-Streilein J. A critical role for alveolar macrophages in elicitation of pulmonary immune fibrosis. Immunology 2000; 101:501-511; PMID:11122454; http://dx.doi.org/10.1046/j.1365-2567.2000.00143.x
37. Gibbons MA, Mackinnon AC, Ramachandran P, Dhaliwal K, Duffin R, Phythian-Adams AT, Van Rooijen N, Haslett C, Howie SE, Simpson AJ, et al. Ly6Chi monocytes direct alternatively activated profibrotic macrophage regulation of lung fibrosis. Am J Respir Crit Care Med 2011; 184:569-581; PMID:21680953; http://dx.doi.org/10.1164/rccm.201010-1719OC